Angle-resolved photoemission study of the hydrogen-adsorbed Cr(110) surface at 80 K

T. Komeda, Y. Sakisaka, and M. Onchi
Department of Chemistry, Faculty of Science, Kyoto University, Kyoto 606, Japan

H. Kato
Photon Factory, National Laboratory for High Energy Physics, Tsukuba-shi, Ibaraki 305, Japan

S. Suzuki
Department of Physics, Faculty of Science, Tohoku University, Sendai 980, Japan

K. Edamoto
Department of Chemistry, Faculty of Science, Tokyo Institute of Technology, Ookayama, Tokyo 152, Japan

Y. Aiura
Institute of Physics, University of Tsukuba, Sakura-mura, Ibaraki 305, Japan
(Received 19 May 1988)

The electronic state of the hydrogen-adsorbed Cr(110) surface at 80 K has been investigated using angle-resolved photoemission spectroscopy. We observed a $p(2\times2)$ low-energy electron-diffraction pattern at ~2 L, and a "streaked" (1×1) pattern along the $[1\bar{1}0]$ azimuth at above 10 L. The photoemission results show that for the $p(2\times2)$ phase an H $1s$-derived state, having a nearly constant binding energy of ~5.5 eV below the Fermi level, is observed in the outer part of the surface Brillouin zone, that is, outside the Cr s-p band projections. [Here 1 langmuir (L)$\equiv10^{-6}$ Torr sec.] On the other hand, for the streaked (1×1) phase, an H $1s$-derived state, split off from the Cr bulk bands, is found at the binding energy of 7.8 eV at $\bar{\Gamma}$ and shows considerable dispersion of ~2.8 eV in the [001] azimuth being consistent with the periodicity of the substrate structure. In addition, a H-induced surface state is found at 2.5 eV at $\bar{\Gamma}$ for both phases. The nature of the Cr-H chemisorption bond is discussed.

I. INTRODUCTION

Metallic chromium, which is an itinerant antiferromagnet, has many interesting physical and chemical properties, such as magnetic phase transition, high corrosion resistivity, and catalytic activities. Concerning the interaction of hydrogen with single-crystal Cr surfaces, there have been quite a few investigations with modern analytical techniques. It is known that the chromium hydride has some phases, Cr_2H, CrH, and CrH_2, dependent on the hydrogen concentration.[1,2]

We previously reported a study of the chemisorbed state of hydrogen on a Cr(110) surface at 300 K by means of low-energy electron diffraction (LEED) and electron-energy-loss spectroscopy (EELS) (electronic transition).[3] At 300 K, exposure of the clean Cr(110) surface to H_2 (<100 L) produced no new spots in the LEED pattern, but caused the slight broadening and intensity decrease of the substrate spots accompanied with a weak background increase, indicating the formation of a disordered adlayer. A H-induced loss peak was observed at ~16 eV in contrast to the Ni(100)-H system,[4] indicating that the hydrogen surface resonance is sharp in the case of the Cr(110)-H system due to strong hybridization with Cr delocalized $3d$ states.

For the light H atom has a high mobility on a metal surface, fairly low temperature is required in order to locate the H atoms on certain lattice sites. Ordered H adlayers at low temperatures have already been detected in the system of H/Ni(110).[5] Since then, ordered overlayer structures have been detected by the method of LEED in the systems of H/Ni(111),[6] H/Fe(110),[7] H/Pd(100),[8] H/Rh(110),[9] and so on.[10]

The use of angle-resolved ultraviolet-photoemission spectroscopy (ARUPS) can give valuable information about the nature of the chemisorption bond of H. Several ARUPS studies have been reported for H/Ti(0001),[11] H/Pd(111),[12-14] H/Pt(111),[12] H/Ni(111),[12,14] H/Ni(100),[15] H/W(110),[16] H/Cu(111),[17] H/Ta(110),[18] H/Ru(0001),[19] and H/Ni(110).[20] In this paper, we report a LEED and ARUPS study of a H/Cr(110) system at 80 K. An ARUPS investigation for clean Cr(110) has already been reported.[21]

II. EXPERIMENT

The Cr(110) single crystal was the same one used in our earlier experiments.[3,21] The clean surface, showing the sharp $p(1\times1)$ LEED pattern with a low background, was prepared by repeated Ar^+-ion sputtering and annealing cycles (details of the surface-cleaning procedure were given in Ref. 21). The amounts of impurities were reduced less than the detection limit of Auger spectroscopy and this corresponds to a coverage of 0.01 monolayers (ML) or less.[3,21] With liquid-N_2 cooling, the crystal

could be cooled to ~80 K. Hydrogen was admitted at 5×10^{-8} to 1×10^{-7} Torr and at the sample temperature of 80 K into the vacuum chamber through a variable-leak valve. The base pressure in the system was 1×10^{-10} Torr.

The ARUPS measurements using synchrotron radiation were performed using a 150° spherical-sector-type analyzer with an acceptance angle of ±1° as described elsewhere.[22–25] The total experimental resolution was 0.1–0.2 eV. The radiation was linearly polarized in the horizontal plane of incidence, and the sample was mounted onto a manipulator with one-axis rotation and x,y,z translation such that the [001] crystal azimuth was oriented horizontally. Therefore, throughout all the experiments, the surface component of the vector potential ($\mathbf{A}$) of the light was in the [001] azimuth. The electron-energy analyzer was capable of angular motion in the $(1\bar{1}0)$ and (001) mirror planes, i.e., along [001] ($\bar{\Gamma}\bar{H}$) and $[1\bar{1}0]$ ($\bar{\Gamma}\bar{N}$) azimuths of the surface Brillouin zone (SBZ). The angle of light incidence, θ_i, from the surface normal could be varied independently.

The parallel component of the detected electron momentum ($k_\parallel$) can be obtained directly from the measured kinetic energy (E_k) and its direction:

$$k_\parallel=[(2m/\hbar^2)E_k]^{1/2}\sin\theta_e\ , \tag{1}$$

where θ_e is the emission angle in the collection plane measured from the surface normal.

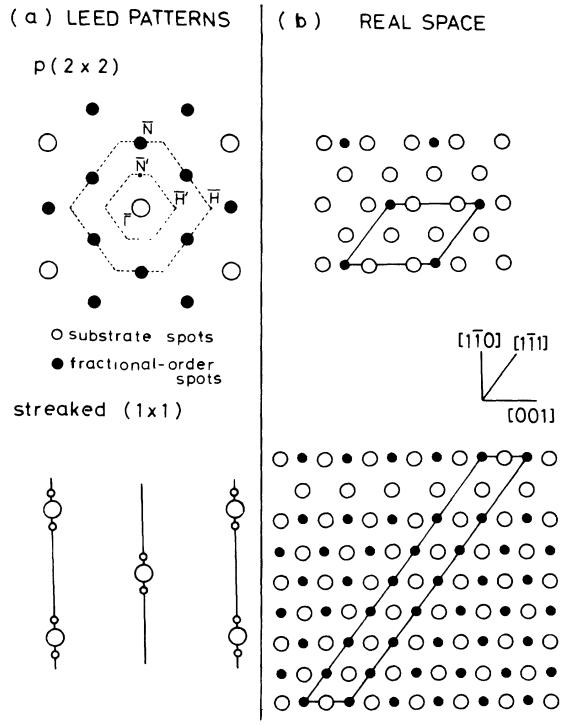

FIG. 1. (a) Schematic LEED patterns of the clean $p(1\times1)$, $p(2\times2)$-H, and (1×1)-H surfaces. (b) Real-space structural models corresponding to the observed LEED patterns (see text).

III. RESULTS AND DISCUSSION

A. LEED

As the Cr(110) clean surface showing the $p(1\times1)$ LEED pattern is exposed to 1–5 L H_2 (1 L$\equiv10^{-6}$ Torr sec) at 80 K, a $p(2\times2)$ pattern is observed as schematically shown in Fig. 1(a). The maximum intensity of the fractional-order spots occurred at ~2 L. As the hydrogen exposure is increased up to ~10 L, the fractional-order spots become weak and finally disappear. The streaks between the integral-order spots along the $[1\bar{1}0]$ azimuth started to be observed at ~7 L. Beyond 10 L the "streaked" (1×1) pattern only is observed: streaks are formed in the $[1\bar{1}0]$ azimuth, the intensity of which seems to be modulated such that the maxima appear in the position of $\frac{1}{8}$ order near the integral-order spots. In the case of the H/Fe(110) system (the same bcc structure as Cr), $p(2\times1)$, (3×1), and $(n\times1)$ $(n\geq4)$ LEED patterns were observed sequentially with increasing hydrogen exposure[7,10] and it has been suggested that the H adatom occupies the twofold hollow (long-bridge) site,[7] the short-bridge site,[26] or recently the quasithreefold site.[27] In the present case the streaky pattern can be considered the formation of $(n\times1)$ structures with large n, where no well-ordered large domains of $(n\times1)$ periodicity exist. In the [001] azimuth the H atoms lie with the periodicity of substrate lattice constant a. Assuming the location of the H atoms in the twofold hollow site on Cr(110), real-space structural models corresponding to the observed LEED patterns are shown in Fig. 1(b) (the on-top adsorption site can be disregarded from the ARUPS results as discussed later). SBZ's for clean Cr(110) and Cr(110)$p(2\times2)$-H are also shown in Fig. 1(a).

B. ARUPS of the clean Cr(110) surface

Before discussing the H-induced features in ARUPS spectra, it is important to understand the off-normal-emission spectra for the clean surface. Figure 2 shows examples of such spectra along the [001]($\bar{\Gamma}\bar{H}$) azimuth measured at the sample temperature of 80 K (antiferromagnetic Cr) and a photon energy of $h\nu=25$ eV. The binding energy (E_B) is referred to the Fermi energy (E_F) of the clean Cr(110) substrate. The $h\nu$ dependence of the $\theta_e=0°$ spectra have been reported earlier[21] and summarized that (1) the feature just below E_F is ascribed to a surface resonance state, (2) emission from the $3d$-like top Σ_1 bulk band is observed at ~1.0 eV for $h\nu=25$–35 eV, which moves with $h\nu$ and the resulting experimental dispersion as well as the location of the band agrees rather well with the calculated one of Asano and Yamashita,[28] (3) emission from the middle Σ_1 band originating from Γ_{12} is observed around 3.0 (3.4) eV for $h\nu=25$ (35) eV, and (4) emission from the $4s$-like lowest Σ_1 band originating from Γ_1 is observed at ~6.0 (6.6) eV for $h\nu=25$ (35) eV.

As seen in Fig. 2, the features move in energy as θ_e is increased. From data like these in Fig. 2, we determined the E-versus-$k_\parallel$ dispersion [$E(k_\parallel)$], using Eq. (1), along the [001] ($\bar{\Gamma}\bar{H}$) and $[1\bar{1}0]$ ($\bar{\Gamma}\bar{N}$) azimuths. The results are summarized in Fig. 3(a). The shaded re-

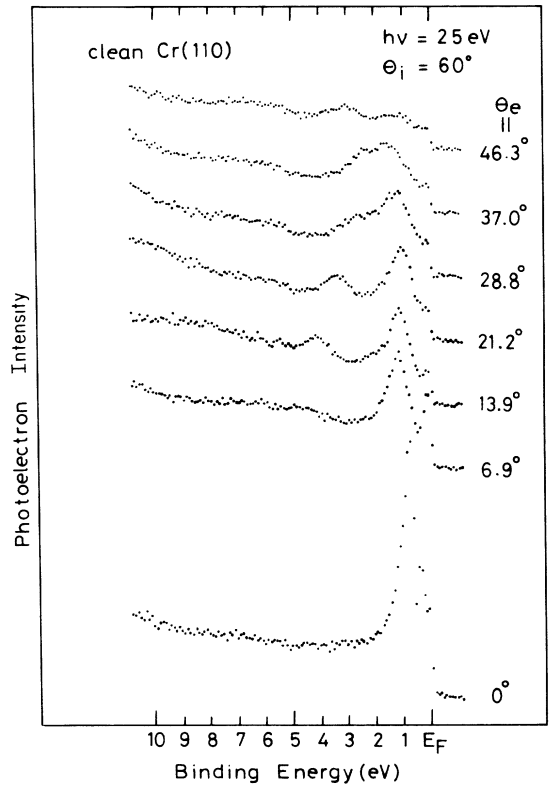

FIG. 2. Angle-resolved photoemission spectra of clean Cr(110) along $\bar{\Gamma}\bar{H}$ ([001]) measured at 80 K, $h\nu=25$ eV, and $\theta_i=60°$ ($A_\parallel$ along [001]).

gion in Fig. 3 is the bottom part of the projection of the calculated bulk s bands onto the bcc(110) SBZ, instead of the sc(110) SBZ, which is convenient for the H-covered surfaces discussed later (the projection was determined by comparing the calculated bands of Cr and Fe and by referring the calculated projection of the Fe bulk bands[29]). The lowest position (Γ_1) has been shifted to 6.7 eV below E_F according to our ARUPS data on clean Cr(110).[21]

Persson and Johansson[30] have measured the ARUPS spectra of clean Cr(110) utilizing Ne I and He I radiations and calculated the band structure of paramagnetic Cr along lines perpendicular to the (110) surface in the ΓNPH plane, i.e., in the ($1\bar{1}0$) mirror plane. From their calculated results, we evaluated the position of the top Σ_1-band emission along the [001] azimuth for $h\nu=25$ eV assuming a free-electron final-state band with an inner potential $V_0=9.8$ eV.[21] The results are shown by the thick solid line in Fig. 3(a), which can be compared to our experimental dispersion. The dispersion of the lowest Σ_1 band for $h\nu=25$ eV [open circles connected by a dashed line in Fig. 3(a)] is similar to the He I results of Persson and Johansson.[30]

C. ARUPS of the $p(2\times2)$-H surface

Now we turn to the discussion of the H-induced features. Figure 4 shows off-normal spectra measured at $h\nu=25$ eV along the [001] ($\bar{\Gamma}\bar{H}'$) azimuth for the Cr(110) surface exposed to ~2 L, where the $p(2\times2)$-H

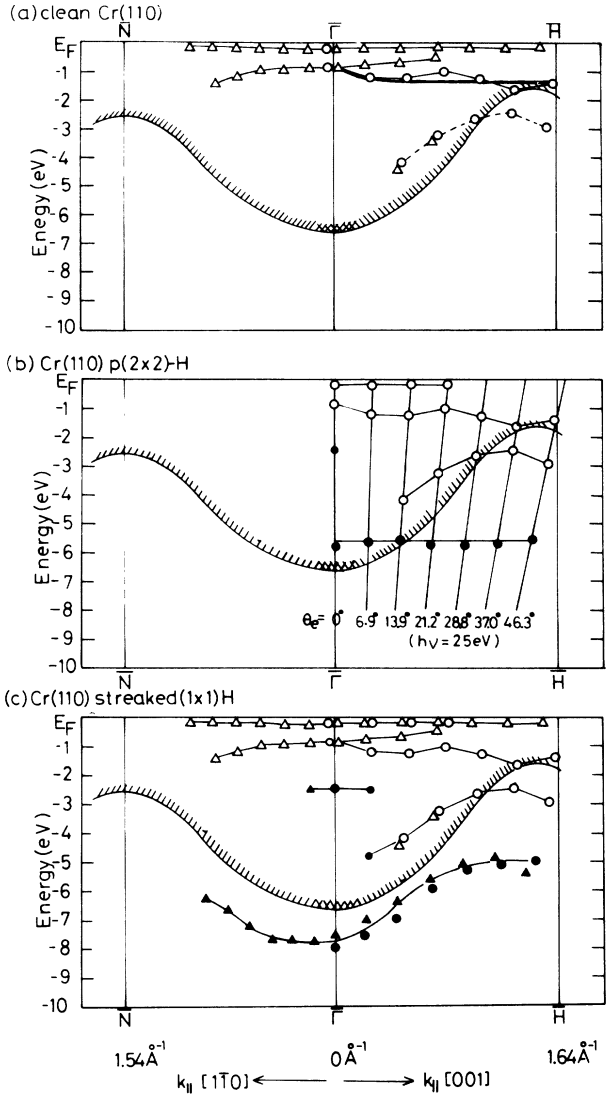

FIG. 3. Dispersion of the peaks in the photoemission spectra for (a) clean Cr(110), (b) Cr(110)$p(2\times2)$-H, and (c) streaked Cr(110)(1×1)-H along [001] and [$1\bar{1}0$]. The shaded region is the bottom part of the projection of the Cr bulk s bands onto the (110) surface (see text). The circles are for $h\nu=25$ eV and triangles are for $h\nu=35$ eV. The solid symbols denote the H-induced states.

LEED pattern was most clearly observed. No H-induced feature split off from the Cr bulk bands appears, but, instead, two H-induced features are observed independent of $h\nu$ and θ_e at constant binding energies of ~2.5 and 5.5 eV, as indicated by solid circles (dispersion, if any, <0.05 eV). The peak positions versus $k_\parallel$ are plotted in Fig. 3(b). The 2.5-eV feature, which is seen only for $\theta_e\sim0°$ (near $\bar{\Gamma}$), is also found for the streaked (1×1)-H phase. We think that the 2.5-eV feature is not ascribed to a H—Cr antibonding state but an H-induced surface state, as discussed later in detail. Here, we confine ourselves to the 5.5-eV feature.

As for the 5.5-eV feature, we can exclude the possibili-

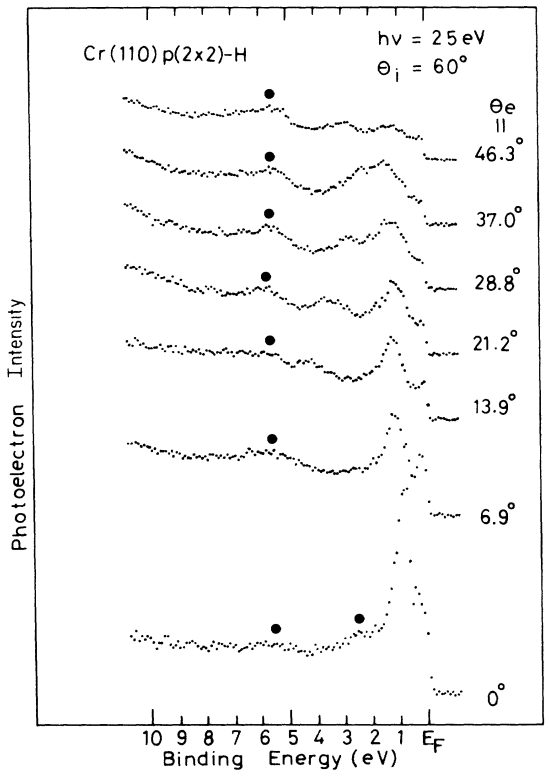

FIG. 4. Angle-resolved photoemission spectra of Cr(110)$p(2\times2)$-H at 80 K along $\bar{\Gamma}\bar{H}'$ ([001]) measured at $h\nu=25$ eV and $\theta_i=60°$ ($A_\parallel$ along [001]). The position of the H-induced state is indicated by solid circles.

ty of detecting an emission being ascribable to the oxygen (and/or H_2O) contamination, because of the cleanness of the surface used and the different peak position [an emission characteristic of the chemisorbed oxygen on Cr(110) is centered at ~6.2 eV (Ref. 31)]. This 5.5-eV H-induced state seen in Fig. 4 ($h\nu=25$ eV) is very weak and broad for $\theta_e<14°$ but becomes sharp and intense beyond $\theta_e\sim21°$. Such change can be explained by a broadening effect due to the hybridization of the H-derived level with the substrate band. As seen in Fig. 3(b), the 5.5-eV state merges into the Cr bulk 4s bands for smaller $k_\parallel$ (i.e., $\theta_e<21°$ for $h\nu=25$ eV), leading to the hybridization broadening. At $\theta_e\sim21°$ for $h\nu=25$ eV it crosses the edge of the bulk bands, and therefore for larger $k_\parallel$ it has nothing to do with such hybridization effects. Considering the large H-H nearest-neighbor distance of 4.98 Å (along $[1\bar{1}1]$) of the $p(2\times2)$-H structure, we expect a small dispersion of the H-derived state. Previously,[20] we have obtained an empirical relationship between the bandwidth (E_{bw}) of the H 1s-derived state and the H-H nearest-neighbor distance (d), comparing the available experimental data, in terms of a tight-binding model. For completeness we repeat it here:

$$E_{bw}=75.8e^{-d/(0.803\ \text{Å})}\ \text{eV}\ , \tag{2}$$

where E_{bw} is given in eV and d in Å. The formula (2) gives $E_{bw}\sim0.1$ eV for $d=4.98$ Å, in agreement with the present observation (<0.05 eV).

The binding energy of the H-derived state at $\bar{\Gamma}$ is smaller for the $p(2\times2)$-H surface associated with a hydrogen coverage of $\Theta=0.25$ ML than for the streaked (1×1) surface with $\Theta\sim0.88$ ML, where the H 1s-derived state is observed at 7.8 eV at $\bar{\Gamma}$ and exhibits a considerable dispersion of 2.8 eV as shown later. Such an upward shift of the H 1s-derived state with decreasing H concentration has been reported for the H/Ni(111) and H/Pd(111) systems,[14] where the 1×1 periodicity of the dispersion of the H-derived band is maintained down to ~30–50% of saturation coverage. The authors of Ref. 14 explained their results by assuming the coverage-dependent attractive H potential, the mobile hydrogen atoms, and the avoided-level-crossing mechanism. Their hypothesis is not, however, very convincing (see Ref. 20). In the present case, we think that the upward shift of the H-derived state for smaller coverage is partly due to the removal of dispersion in the H level.

D. ARUPS of the streaked (1×1)-H surface

As stated above, exposure of the clean Cr(110) surface to hydrogen above ~10 L at 80 K leads to the formation of the streaked (1×1) structure: streaks are formed along the $[1\bar{1}0]$ azimuth. Figures 5 and 6 show off-normal spectra of such a streaked (1×1)-H surface ob-

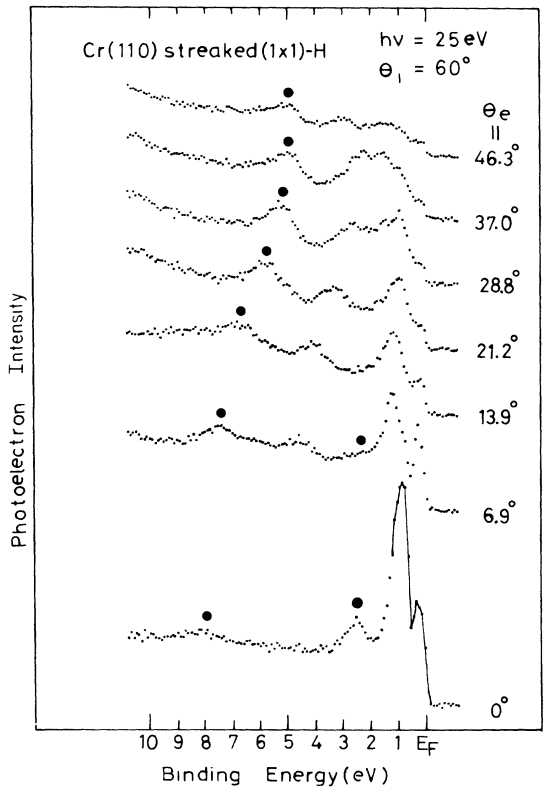

FIG. 5. Angle-resolved photoemission spectra of streaked Cr(110)(1×1)-H at 80 K along [001] measured at $\theta_i=60°$ ($A_\parallel$ along [001]) and $h\nu=25$ eV. The position of the H-induced state is indicated by solid circles.

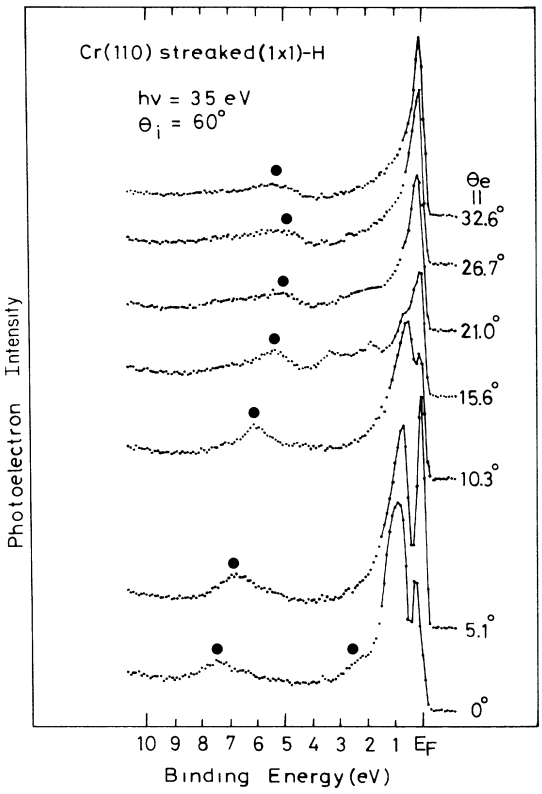

FIG. 6. Same as in Fig. 5, except $h\nu$ is now changed to 35 eV.

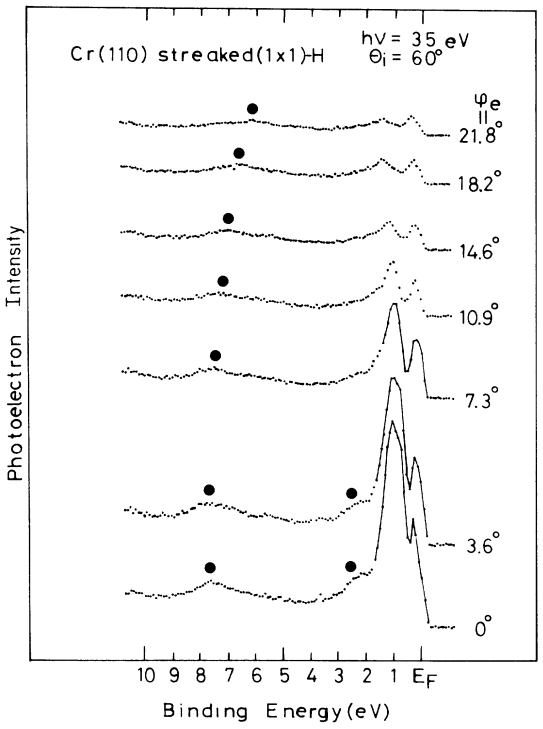

FIG. 7. Angle-resolved photoemission spectra of streaked Cr(110)(1×1)-H at 80 K along [1$\bar{1}$0] measured at $h\nu=35$ eV and $\theta_i=60°$ ($A_\parallel$ along [001]). The position of the H-induced state is indicated by solid circles.

tained after exposure of 40 L, measured along the [001] azimuth at $h\nu=25$ eV in Fig. 5 and $h\nu=35$ eV in Fig. 6. There was no change in the spectra with further exposures. For comparison, the clean-surface spectra measured at the same experimental configuration are shown by solid lines. In Fig. 7 we show the off-normal spectra of the same streaked (1×1)-H surface along the [1$\bar{1}$0] azimuth. By comparing the spectra of streaked (1×1)-H with the clean-surface spectra, H-induced features can be identified. The H-induced features are indicated by solid circles in Figs. 5–7. This identification is confirmed by the fact that such two-dimensional states should have their energies in a spectrum independent of $h\nu$ if $k_\parallel$ is held fixed. Figure 8 shows the $h\nu$ dependence of the spectra at (a) $k_\parallel=0$ ($\bar{\Gamma}$) and (b) $k_\parallel=1.03$ Å^{-1} in the [001] azimuth ($k_\parallel=\frac{2}{3}\bar{\Gamma}\bar{H}$ in the clean-surface SBZ). As expected, the H-induced features, which are identified above, stay at fixed binding energies of 7.8 and 2.5 eV for $k_\parallel=0$ and 5.5 eV for $k_\parallel=1.03$ Å^{-1} when $h\nu$ is changed.

Figure 3(c) shows peak positions versus $k_\parallel$ obtained from series of off-normal-emission spectra in Figs. 5–7 for $h\nu=25$ eV (circles) and $h\nu=35$ eV (triangles) in two directions corresponding to $\bar{\Gamma}\bar{H}$ and $\bar{\Gamma}\bar{N}$ directions of the clean-surface SBZ. As seen in Figs. 3 and 5, the substrate emission features are almost unchanged by H adsorption, especially in energy positions. The surface-resonance feature just below E_F is reduced by H adsorption for $k_\parallel=0$ (normal emission), but this reduction is not clear for $k_\parallel\neq0$ (off-normal-emission case). The weak 4.8-eV feature in the $\theta_e=6.9°$ clean-surface spectrum for $h\nu=25$ eV is enhanced by H adsorption (see Fig. 5). This feature can be ascribed to the Cr bulk band (s-like lowest Σ_1 band), not to a surface-related state because a corresponding feature is not seen in the $h\nu=35$ eV spectra (Fig. 6).

The adsorption of H produced two features in normal emission, at 7.8 and 2.5 eV below E_F. As shown in Fig. 3(c), the 7.8-eV state is present at 1.1 eV below the bulk bands and disperses upward by ~2.8 eV as $k_\parallel$ is changed along the [001] azimuth perpendicular to the streaks. This dispersion along [001] exhibits the correct periodicity for the streaked (1×1)-H structure, i.e., π/a, where a is the lattice constant of Cr. The empirical formula (2) gives $E_{bw}=2.1$ eV for $d=a=2.88$ Å, in rough agreement with experiment. Interestingly, the 7.8-eV state shows considerable dispersion in the [1$\bar{1}$0] azimuth parallel to the streaks also. There is no well-ordered large domains of (n×1) which have higher periodicity along the streak direction. We can reconcile the dispersion of the 7.8-eV H-induced state along [1$\bar{1}$0] with the streaked (1×1) structure by assuming the mobile hydrogen atoms as proposed in Ref. 14. In other words, this overlayer structure is essentially the (1×1)-H in the electronic viewpoint. Note that in our structural model (Fig. 1), as a statistical average, only one of the eight [001] rows is missing. The 2.5-eV H-induced feature does not

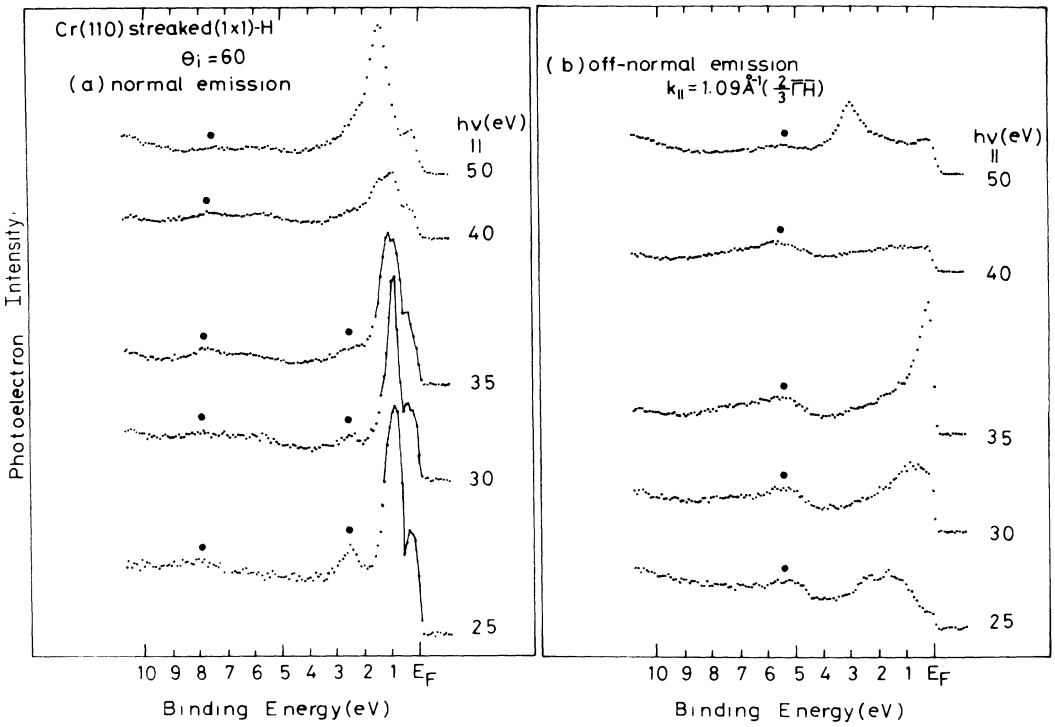

FIG. 8. $h\nu$ dependence of angle-resolved photoemission spectra for streaked Cr(110)(1×1)-H measured at $\theta_i = 60°$ ($A_\parallel$ along [001]): (a) normal emission and (b) off-normal emission ($k_\parallel = 1.03$ Å^{-1} along [001] at 8 eV). The positions of the H-induced states are indicated by solid circles.

disperse with $k_\parallel$ and can only be seen for small emission angles (i.e., $k_\parallel < 0.2$ Å^{-1}). This 2.5-eV feature exists in the s-d-hybridization gap at $\bar{\Gamma}$ in Cr (see, e.g., the even-symmetry bands along [001] in Fig. 7 of Ref. 21).

Such a two-peak UPS spectrum has also been reported for H/Ti(0001) [1.3 and 6.9 eV below E_F at $\bar{\Gamma}$ (Ref. 11)], H/Ta(110) [2.2 and 6.5 eV at $\bar{\Gamma}$ (Ref. 18)], and H/Ru(0001) [3.7 and 8.1 eV at $\bar{\Gamma}$ (Ref. 19)]. Our data for streaked (1×1)-H resemble those for H/Ti(0001) reported by Feibelman *et al.*[11] in many points, e.g., the upper H-induced state is dispersionless and observable only around $\bar{\Gamma}$ and the lower H-induced state is split off from the substrate bands and shows upward dispersion. Feibelman *et al.*[11] also calculated the electronic surface band structure of Ti(0001)-H for various Ti—H bond lengths and surface geometries in order to find the geometrical structure by fitting the calculated results to the ARUPS data. The Ti—H bond length was chosen to be 1.75–1.90 Å. Their calculation shows that (1) the upper and lower H-induced states correspond to the antibonding and bonding combinations of H 1s and Ti 3d,4s orbitals, and the splitting of the bonding-antibonding pair is very sensitive to the Ti—H bond length, (2) the H-induced states appear for all sites (both underlayer and overlayer sites) except the on-top site, (3) for H in the on-top site none of the H-induced states is split off from the bulk bands (and, therefore, should not be observed) because the H 1s and Ti 3d overlap is very small, and (4) the intrinsic d-like surface state is quenched by H in the overlayer site but not strongly perturbed by H in the underlayer site. Although a similar calculation has not been performed for the H/Cr(110) system, it is useful to compare the results of Feibelman *et al.*[11] with our experimental results in a qualitative way.

According to the results of Feibelman *et al.*,[11] we may regard the two H-induced states, at ~2.5 and 7.8 eV at $\bar{\Gamma}$, as an occupied pair of the H 1s—Cr 3d,4s antibonding and bonding states. However, as stated before, the similar 2.5-eV feature is also found for the $p(2\times2)$-H phase, where the other feature exists at 5.5 eV ($\bar{\Gamma}$) instead of 7.8 eV, i.e., there is no split-off state. Therefore, the 2.5-eV state cannot be attributed to an H—Cr antibonding state. We consider that the 7.8-eV state is an H 1s—Cr bonding state, but the 2.5-eV state is an extrinsic H-induced surface state, in contrast to the model of Feibelman *et al.*[11] According to the results of Chan and Louie,[32] such an extrinsic surface state is an intrinsic surface state shifted in energy as a consequence of changes in the surface potential due to the presence of H or an additional surface state being characteristic of H in the subsurface sites. We cannot decide which model is correct. In other words, we cannot easily reject the subsurface model, since (1) the Cr(110) surface does not have a subsurface tetrahedral site, but does have a subsurface quasioctahedral site, and (2) our previous study of H adsorption on Cr(110) at 300 K (Ref. 3) suggests that hydrogen is rapidly penetrated into the Cr selvage lattice. The calculation of Chan and Louie[32] concluded the lack of d-like character in the bonding state at $\bar{\Gamma}$ for H at the octahedral site from a simple geometrical reason. However, this is in contrast

to our data. As will be discussed below, the bonding character is mainly d-like at $\bar{\Gamma}$.

Because the Cr-H distance given by adding the Cr metallic radius (1.25 Å) to the H covalent radius (0.32 Å) is ~ 1.6 Å and the distance in CrH or CrH_2 is 1.7 Å,[1] we assume that the Cr—H bond length is 1.6–1.7 Å. This is not a poor choice, and can be compared with the Ti—H bond length of 1.8–1.9 Å used in Ref. 11. Following Feibelman *et al.*[11] we rule out the on-top site for H on Cr(110), since the H-induced split-off state exists. Other overlayer sites (e.g., the long-bridge site, short-bridge site, and quasithreefold site) are spectroscopically acceptable, and it is difficult to decide which geometrical structure is correct from photoemission data alone.

Finally, we wish to discuss the Cr—H bonding character. Previous theoretical workers have discussed the relative importance of metal (Ni, Pd) s, p, and d orbitals in H chemisorption, but there is still a controversy regarding this problem (see Ref. 20 and other related references therein). The photoemission measurements give one the potential to identify the bonding character, i.e., distinguish the contribution of distinctive atomic orbitals to the bonding state. This technique has to rely on the relative magnitude of the atomic photoionization cross sections (σ's) of H 1s and metal d electrons. It should be noted that, contrary to what was tacitly assumed, the atomic H 1s cross section is comparable to the metal d cross section per electron at $h\nu \sim 20$–40 eV, as has been suggested in Ref. 20. Therefore, we have to be very cautious of treating the data.

The θ_e dependence of the H 1s split-off feature is seen in Figs. 5 and 6 (along [001], $h\nu=25$ and 35 eV, respectively) and Fig. 7 (along $[1\bar{1}0]$, $h\nu=35$ eV). The $h\nu$ dependence is shown in Fig. 8 [(a) for $k_{\parallel}=0$ and (b) for $k_{\parallel}=1.03$ Å^{-1}]. This H 1s split-off state has a measured width (full width at half maximum) of ~ 1.1 eV, which is considerably smaller than that (~ 1.5 eV) for H/Ni(110) (Ref. 20) and H/Ni(111) (Refs. 12 and 14). We need to know $\sigma(\omega)$ for H 1s (Ref. 33) and Cr 3d to obtain information about the nature of the bonding state from our data. Unfortunately, the experimental atomic Cr 3d cross section is not known for $h\nu=20$–40 eV. Instead, we use the experimentally determined atomic Mn 3d cross section.[34] This is not a poor choice. Figure 9 shows the atomic photoionization cross sections (per electron) for H 1s and Mn 3d [denoted σ_s(H) and σ_d(Mn)] deduced from Refs. 33 and 34, respectively. We note that σ_s(H) has a maximum at $h\nu \sim 18$ eV and then decreases slowly with $h\nu$, while σ_d(Mn) peaks at $h\nu \sim 30$ eV. From Fig. 9 the ratio $\sigma_d(\mathrm{Mn})/\sigma_s(\mathrm{H})$ is found to be ~ 0.7 at $h\nu=25$ and ~ 2 at $h\nu=35$ eV. As seen in Fig. 8, the H 1s split-off state is not most visible at around $h\nu=30$ eV, contrary to what is expected from the σ(Mn 3d) curve. Its intensity is rather constant for $h\nu=25$–35 eV, and then decreases slowly as $h\nu$ increases. We can say that the H 1s split-off state does not have a 100% s character, but a considerable (50–60%) d character [see curves (2)–(4) in Fig. 9]. Here, we neglect the crossterms in the square of the matrix element. Figures 5–7 show that the H 1s split-off state is more pronounced away from $\bar{\Gamma}$ for $h\nu=25$ eV, but the reverse is true for $h\nu=35$ eV. These

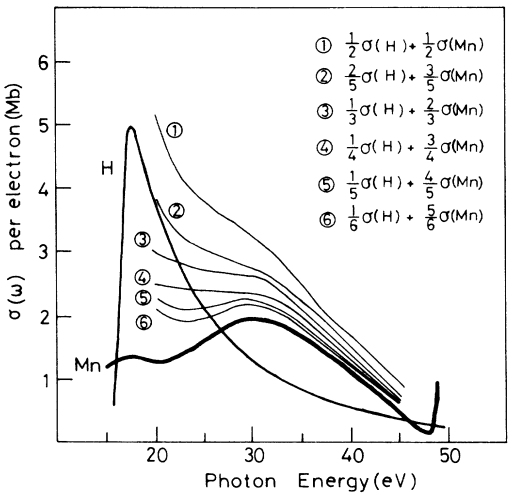

FIG. 9. Experimentally determined atomic photoionization cross sections (per electron) for H 1s [σ(H)] and Mn 3d [σ(Mn)] deduced from Refs. 33 and 34, respectively (see text). Curves (1)–(6) represent the sum of σ(H) and σ(Mn): (1) $\frac{1}{2}\sigma(\mathrm{H})+\frac{1}{2}\sigma(\mathrm{Mn})$, (2) $\frac{2}{5}\sigma(\mathrm{H})+\frac{3}{5}\sigma(\mathrm{Mn})$, (3) $\frac{1}{3}\sigma(\mathrm{H})+\frac{2}{3}\sigma(\mathrm{Mn})$, (4) $\frac{1}{4}\sigma(\mathrm{H})+\frac{3}{4}\sigma(\mathrm{Mn})$, (5) $\frac{1}{5}\sigma(\mathrm{H})+\frac{4}{5}\sigma(\mathrm{Mn})$, and (6) $\frac{1}{6}\sigma(\mathrm{H})+\frac{5}{6}\sigma(\mathrm{Mn})$.

findings put us in a dilemma if we believe that the photoionization cross sections for s electrons are generally much weaker than d electrons. This is not the case. If we admit that $\sigma_d < \sigma_s$ at $h\nu=25$ eV and $\sigma_d > \sigma_s$ at $h\nu=35$ eV (see Fig. 9), our findings lead to a conclusion that the s character of the split-off state increases going away from $\bar{\Gamma}$, contrary to the theoretical results.[32] In other words, the Cr—H bonding state is mainly d-like at around $\bar{\Gamma}$ and mainly s-like near the zone boundary.

An Anderson-Newns–type initial-state broadening has nothing to do with the reduction in intensity of the H split-off state near $\bar{\Gamma}$ for $h\nu=25$ eV, since this state is 1.1 eV off from the bottom of the Cr bulk band. The situation is not clear for H/Ni(110),[20] H/Ni(111)[12–14] and H/Pd(111),[12–14] where the H state is only 0.2 eV or less off from the respective bulk band (the position of the H state at $\bar{\Gamma}$ (the bottom of the s band) is 9.0 (8.8) eV both for H/Ni(110) and H/Ni(111), and 7.9 [8.0 (Ref. 35)] eV for H/Pd(111)). On Cr(110) the H 1s split-off state is narrower than on Ni(110) and Ni(111) [1.1 eV versus 1.5 eV (Refs. 20 and 14)]. Muscat and Newns[36] showed in their theoretical work of H chemisorption on Ni, Pd, and Pt that the H 1s–metal d interaction makes the H-jellium resonance narrow. From all the results, we can say that the admixture of 3d states into the H-induced state is stronger for Cr(110) than for Ni(110) and Ni(111), in agreement with our previous electronic EELS study.[3]

Here some caution should be exercised. No matter how properly the crossterms in the square of the matrix element are allowed for, our results are still tentative. A major problem with the above reasoning is that for many atoms the σ data are neither highly reliable nor available. Since σ_d is not always larger than σ_s, we emphasize that

all the previous arguments to obtain information about the bonding character should be reexamined by using reasonable σ_s and σ_d.

IV. CONCLUDING REMARKS

At 80 K, LEED shows two ordered hydrogen overlayer structures on Cr(110): $p(2\times2)$ at low coverage and streaked (1×1) at high coverage. In both phases, AR-UPS shows two H-induced states. One is an extrinsic H-induced surface state which exists at $E_B=2.5$ eV and only around $\bar{\Gamma}$ for both phases. The other is an H $1s$—Cr bonding state (the H—Cr antibonding state is considered to be above E_F). In the $p(2\times2)$-H phase it exists at $E_B=5.5$ eV at $\bar{\Gamma}$ and shows no dispersion. On the other hand, in the streaked (1×1)-H phase the H $1s$ state is split off from the Cr bulk band. It exists at $E_B=7.8$ eV at $\bar{\Gamma}$ and shows considerable dispersion along both [001] and $[1\bar{1}0]$ azimuths (perpendicular and parallel to the streak direction, respectively). To explain the dispersion along $[1\bar{1}0]$, we assume a mobility of the adsorbed H atoms. The upward shift of the H $1s$ bonding state at $\bar{\Gamma}$ for smaller H concentration can mainly be ascribed to the removal of dispersion in the H level. There is no direct evidence for subsurface H on Cr(110) at 80 K, but it is difficult to extract a definitive geometrical structure based only on the photoemission spectra.

From the $h\nu$ and θ_e dependence of the H $1s$ split-off feature for the streaked (1×1)-H, we conclude that Cr—H bonding state has a 50–60 % d-like character at $\bar{\Gamma}$ and becomes s-like going away from $\bar{\Gamma}$. However, our reasoning depends entirely on the reliability of $\sigma(\omega)$ data of H $1s$ and metal d electrons and neglects the crossterms in the square of the matrix elements. We stress that the atomic H $1s$ photoionization cross section is not much smaller than, but is comparable to, the metal d cross section per electron at $h\nu\sim20$–40 eV.

ACKNOWLEDGMENTS

We are pleased to thank the staff of the Photon Factory, National Laboratory for High Energy Physics, Ibaraki, particularly T. Miyahara, for their excellent support. This work has been performed under the approval of the Photon Factory Program Advisory Committee (Proposal No. 86-150).

[1]C. A. Snavely and D. A. Vaughan, J. Am. Chem. Soc. **71**, 313 (1949).

[2]*Hydrogen in Metals I and II,* Vols. 28 and 29 of *Topics in Applied Physics,* edited by G. Alefeld and J. Volkl (Springer, New York, 1978).

[3]Y. Sakisaka, H. Kato, M. Nishijima, and M. Onchi, Solid State Commun. **36**, 353 (1980); H. Kato, Y. Sakisaka, M. Nishijima, and M. Onchi, Surf. Sci. **107**, 20 (1981).

[4]H. Kato, Y. Sakisaka, M. Nishijima, and M. Onchi, Phys. Rev. B **22**, 1709 (1980).

[5]T. N. Taylor and P. J. Estrup, J. Vac. Sci. Technol. **11**, 244 (1974).

[6]K. Christmann, R. J. Behm, G. Ertl, M. A. Van Hove, and W. H. Weinberg, J. Chem. Phys. **70**, 4168 (1979).

[7]F. Bozso, G. Ertl, M. Grunze, and M. Weiss, Appl. Surf. Sci. **1**, 103 (1977); R. Imbihl, R. J. Behm, K. Christmann, G. Ertl, and T. Matsushima, Surf. Sci. **117**, 257 (1982).

[8]R. J. Behm, K. Christmann, and G. Ertl, Surf. Sci. **99**, 320 (1980).

[9]K. Christmann, M. Ehsasi, W. Hirshwald, and J. H. Block, Chem. Phys. Lett. **131**, 192 (1986).

[10]K. Christmann, Ber. Bunsenges. Phys. Chem. **90**, 307 (1986).

[11]P. J. Feibelman, D. R. Hamann, and F. J. Himpsel, Phys. Rev. B **22**, 1734 (1980).

[12]W. Eberhardt, F. Greuter, and E. W. Plummer, Phys. Rev. Lett. **46**, 1085 (1981).

[13]W. Eberhardt, S. G. Louie, and E. W. Plummer, Phys. Rev. B **28**, 465 (1983).

[14]F. Greuter, I. Strathy, E. W. Plummer, and W. Eberhardt, Phys. Rev. B **33**, 736 (1986).

[15]P. A. Dowben and Y. Sakisaka (unpublished).

[16]G. B. Blanchet, N. J. DiNardo, and E. W. Plummer, Surf. Sci. **118**, 496 (1982).

[17]F. Greuter and E. W. Plummer, Solid State Commun. **48**, 37 (1983).

[18]V. Murgai, S. L. Weng, M. Strongin, and M. W. Ruckman, Phys. Rev. B **28**, 6116 (1983).

[19]P. Hofmann and D. Menzel, Surf. Sci. **152&153**, 382 (1985).

[20]T. Komeda, Y. Sakisaka, M. Onchi, H. Kato, S. Masuda, and K. Yagi, Phys. Rev. B **36**, 922 (1987).

[21]Y. Sakisaka, T. Komeda, M. Onchi, H. Kato, S. Suzuki, K. Edamoto, and Y. Aiura, Phys. Rev. B **38**, 1131 (1988).

[22]Y. Sakisaka, T. Komeda, M. Onchi, H. Kato, S. Masuda, and K. Yagi, Phys. Rev. Lett. **58**, 733 (1987).

[23]Y. Sakisaka, T. Komeda, M. Onchi, H. Kato, S. Masuda, and K. Yagi, Phys. Rev. B **36**, 6383 (1987).

[24]H. Kato, T. Ishii, S. Masuda, Y. Harada, T. Miyano, T. Komeda, M. Onchi, and Y. Sakisaka, Phys. Rev. B **32**, 1992 (1985).

[25]Y. Sakisaka, T. Komeda, T. Miyano, M. Onchi, S. Masuda, Y. Harada, K. Yagi, and H. Kato, Surf. Sci. **164**, 220 (1985).

[26]A. M. Baro and W. Erley, Surf. Sci. **112**, L759 (1981).

[27]W. Moritz, R. Imbihl, R. J. Behm, G. Ertl, and T. Matsushima, J. Chem. Phys. **83**, 1959 (1985).

[28]S. Asano and J. Yamashita, J. Phys. Soc. Jpn. **23**, 714 (1967).

[29]Ed Caruthers and L. Kleinman, Phys. Rev. B **10**, 376 (1974).

[30]P. E. S. Persson and L. I. Johansson, Phys. Rev. B **33**, 8814 (1986); **34**, 2284 (1986).

[31]T. Komeda, Y. Sakisaka, M. Onchi, H. Kato, S. Suzuki, K. Edamoto, and Y. Aiura, Phys. Rev. B **38**, 7345 (1988).

[32]C. T. Chan and S. G. Louie, Solid State Commun. **48**, 417 (1983); Phys. Rev. B **30**, 4153 (1984).

[33]D. A. L. Kilcoyne, C. M. McCarthy, S. Nordholm, N. S. Hush, and P. R. Hilton, J. Electron. Spectrosc. Relat. Phenom. **36**, 153 (1985).

[34]M. O. Krause, T. A. Carlson, and A. Fahlman, Phys. Rev. A **30**, 1316 (1984).

[35]D. Chandesris, G. Krill, G. Maire, J. Lecante, and Y. Petroff, Solid State Commun. **37**, 187 (1981).

[36]J. P. Muscat and D.M. Newns, Phys. Rev. Lett. **43**, 2025 (1979); Surf. Sci. **89**, 282 (1979).